Results of Acoustic Tests of a Prop-Fan Model

F. B. Metzger* and P. C. Brown†
United Technologies Corporation, Windsor Locks, Connecticut

Results of acoustic tests in a low-speed open-jet anechoic wind tunnel are presented for a counter-rotation prop-fan model. The model tested had five front and five rear rotor blades with swept planform. Noise spectra are presented showing the influence of operating and configuration variables such as 1) power absorption, 2) tip speed, 3) rotor-rotor spacing, 4) power split between the front and rear blade rows, 5) variation of the rpm ratio between front and rear blade rows, 6) tractor pusher (pylon effects), and 7) angle of attack. In addition to model scale results, calculated levels derived from tests are presented showing the influence of the above variables on effective perceived noise level of a 13.1 ft diam propfan at a flyover distance of 1500 ft. It was found that the strongest effects are caused by variations in tip speed and power absorption. A significant finding was that there is an optimum operating tip speed for minimum noise for a given power absorption. Effects of other parametric variations are generally small but measurable. In order to miminize noise to meet airplane certification limits, operation at moderate tip speeds and power absorption is shown to be desirable. Accuracy of predicted effective perceived noise level is shown to be good with the best accuracy in the 590 to 670 ft/s tip speed range.

Nomenclature

B = number of blades on one rotor
BPF = blade passage frequency, $B \times$ RPM/60
C = pylon chord
D = prop-fan diameter in ft
EPNdB = effective perceived noise level in decibels
M = mach number
N = an integer
SHP = shaft horsepower

Introduction

THE prop fan is an advanced technology turboprop concept incorporating many swept blades. For several years, the single-blade row version has been under development. High fuel efficiency relative to turbofans was the reason for interest in the concept. More recently, the counter-rotation (two-blade rows) version of the prop fan has received attention because of its even greater efficiency. This paper presents initial results from an acoustic test of a model prop fan, the CRP-X1, designed by Hamilton Standard.

The characteristics of the CRP-X1 and its installation in the United Technologies Research Center Acoustic Research Tunnel are shown in Fig. 1. The CRP-X1 model has five blades on the front row and five on the rear. The blade tip sweep is 34 deg. It was designed for tractor operation, although, as shown in Fig. 1, it was run in the pusher mode with a pylon upstream. Design tip speed at both takeoff and cruise is 750 ft/s. However, the performance of the CRP-X1 is satisfactory at tip speeds from 600 to 800 ft/s, and this range was explored in the test program. The design takeoff condition was 88.7 SHP/D^2 at $M = 0.2$ sea level. For the test program, all of the test data were acquired at $M = 0.26$. The test facility could not be operated at the 0.72 design cruise Mach number.

Figure 1 shows the arrangement of the drive rig and propfan in the pusher mode. On the left side of the photograph is the nozzle that supplies air to the tunnel. Part of the anechoic treatment on the walls, floor, and ceiling of the facility can be seen in the background.

The microphones in the foreground are mounted at 0.8 diam tip clearance. They were deployed in this test for reference purposes at the same location as microphones used in earlier testing of single-rotation prop fans. The data from these microphones will not be discussed in this report. All of the data to be discussed were obtained in the far field at microphones deployed axially and transversely around the prop-fan axis. Some of the transverse microphones can be seen in Fig. 1 on the opposite side of the prop-fan axis at the upper-right corner of the photograph.

The parameters investigated in the test program are shown in Fig. 2. Tests were conducted 1) in the tractor mode with no pylon upstream and a short spinner ahead of the blades, and 2) in the pusher mode with a pylon and forebody simulating an engine upstream. Tests were conducted at two angles of attack. Most of the testing was conducted at a 0 deg angle of attack. However, other data were obtained with the test rig pitched down 4 deg to simulate takeoff or approach angle-of-attack effects. The downtilt was used for the simulation because of the tunnel geometry. The flow centerline of the tunnel was nearer the floor than the ceiling; therefore, microphones were deployed near the ceiling to obtain data in the far field. The overhead microphones simulate those that would be located on the ground under the flight path and on the sideline for an airplane flyover.

Tests were conducted with different spacing between the two rotors. The definition for rotor spacing is the distance between the pitch change axes divided by the diameter D of the propfan. In the pusher mode, tests were also conducted with different spacings between the trailing edge of the pylon and the leading edge of the front rotor. The definition used for this spacing is the distance between the leading edge of the front rotor and the trailing edge of the pylon (when the prop-fan front rotor is set at its cruise blade angle) divided by pylon chord. The pylon chord C used in the calculation is that closest to the prop-fan leading edge.

In some of the following information, the power split between the front and rear rotor will be discussed. In every case, the percentage of total power absorbed by the front rotor divided by the percentage of total power absorbed by the rear rotor will be used to describe the power split. Unequal rpm between the front and rear rotors was also explored. Here, the convention used for the following discussion is the ratio of the front rotor rpm to that of the rear rotor.

Received Aug. 10, 1987; revision received Sept. 23, 1987.

*Chief of Propulsion Analysis, Hamilton Standard Division. Associate Fellow AIAA.

†Vibration Analysis Engineer, Hamilton Standard Division.

24½ inch rotor diameters
5 blades on front and rear row
34° tip sweep
234 activity factor per blade
Tractor design
750 ft/sec design tip speed
0.24 front hub to tip ratio
0.275 rear hub to tip ratio
88.7 takeoff Shp/D² at 0.2 Mn sea level
37.2 cruise Shp/D² at 35K ft alt at 0.72 Mn

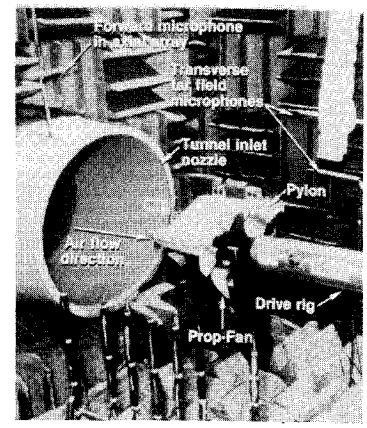

Fig. 1 Configuration and test facility installation.

Type of installation	Tractor and pusher (pylon)
Tip speed	600 to 800 ft/sec
Tunnel speed	0.26 Mach number
Power loading	20 to 136 Shp/D²
Angle-of-attack	0° and 4°
Spacing between rotors	0.257, 0.363 and 0.461 Prop-Fan diameters
Spacing between pylon and front rotor	0.1 and 0.2 pylon chords
Power split between front and rear rotor	75/25 to 48/52 front/rear
RPM ratio (front/rear)	0.8 to 1.2

Fig. 2 Parameters investigated in CRP-X1 test.

All testing was conducted in the United Technologies Research Center Acoustic Research Tunnel. This facility is an open-jet tunnel with inlet flow drawn from ambient and turbulence of the jet controlled by screens upstream of the test section. The tunnel is driven by a centrifugal fan connected to the tunnel outlet by a diffuser that includes a fan silencer duct section.

Figure 3 shows the location of all of the microphones used in this report. The axial microphones are labeled A1 – A7. Microphone N1, installed flush on the inside surface of the nozzle, is used to obtain far forward data. The transverse microphones are labeled T1 – T6. Microphones T1 – T3 are on the side of the prop-fan drive ring closest to the observer in Fig. 3. Microphones T4 – T6 are on the opposite side of the drive rig.

Figure 3 shows the far-field microphone locations and the typical character of the noise spectrum obtained in the Acoustic Research Tunnel. Sample spectra from microphones A1 – A7 for a typical test condition are shown. It can be seen that the tones stand out above the broadband noise so that a minimum of 10 harmonics at every directivity can easily be resolved. For the data shown in the figure, the front rotor rpm was slightly higher than that of the rear rotor. This leads to the double peaks at some of the harmonics in the figure. For the slightly different front and rear rotor rpms, the data were processed by integrating the energy around the rpm harmonics in order to establish the level that would be obtained if the two rotors were running at the same rpm.

The data from the test program were recorded on multichannel tape recorders and then played back through a 400 line spectrum analyzer and digitized on magnetic tape. This tape was then processed on a mainframe computer to extract only the tone levels in the spectrum. Broadband noise was not included as it is known from propeller tests that it cannot be scaled like tone data. The method developed by Schlinker and Amiet[2] was used to correct for the effects of the shear layer that exists between the prop-fan model and the microphones in the far field. A constant radius correction was applied to normalize the differences in distance that exist between the prop fan and various microphones. In addition, this data was used to synthesize an effective perceived noise level for a scaled prop fan. For convenience, all of the scaled effective perceived noise levels assume a 13.1 ft diam prop fan and a flyover distance of 1500 ft. It is assumed that the flyover Mach number is the same as the tunnel test Mach number, i.e., 0.26.

Summary of Test Results

Results of the test program are presented in several ways in this section. First, the fore and aft directivity of harmonics of blade passage frequency ($N \times B \times RPM/60$) are presented as though levels were measured along a line parallel to the tunnel centerline with the effects of tunnel shear layer removed analytically. Second, these same harmonics are presented for the transverse microphone array assuming a constant radial distance to the microphones. Third, the data is scaled and processed to estimate free-field (no ground reflection) effective perceived noise level for a single counter-rotating prop fan, 13.1 ft in diameter, flying at $M = 0.26$ at an altitude of 1500 ft.

Tractor Data at 0 Deg Angle of Attack

Figure 4 shows the effect of power on noise level at constant tip speed. The plot at the left is for a condition of 63.78 SHP/D^2, whereas the figure at the right is for 86.7 SHP/D^2. The tip speed for the two cases is approximately the same. Also, the power split between the front and rear rotors is about the same. For example, the condition at the left had a power split of 59% power on the front rotor and 41% power on the rear rotor. The figures show the sound pressure level as a function of emission angle, i.e., the angle of noise radiation relative to the axis of rotation forward of the plane of rotation. The first four blade passage frequency harmonics and also the tenth harmonic of blade passage frequency are shown. Between the fourth and tenth harmonic the levels decrease, but the details of the directivity become very difficult to interpret due to the limited number of micophones in the axial array. Therefore, in the rest of this paper, only the first four harmonics of blade passage frequency plus the tenth harmonic will be presented. The tenth harmonic is included as an example of the general level and character of the high-frequency noise. In Fig. 4, it can be seen that the level of the first four harmonics of blade passage frequency increase with power loading. The tenth harmonic does not appear to change dramatically.

Figure 5 shows the effect of tip speed at constant power loading. In this case, the power loading is approximately 87 SHP/D^2. Tip speed changes from 652 to 716 ft/s. The blade passage frequency level is shown to increase as the tip speed increases. The other harmonics also change in level with the tenth harmonic increasing a noticeable amount.

Figure 6 shows a scaled generalization of the data available from the equal rpm 0 deg angle-of-attack tractor testing. The levels shown are free-field effective perceived noise level for a

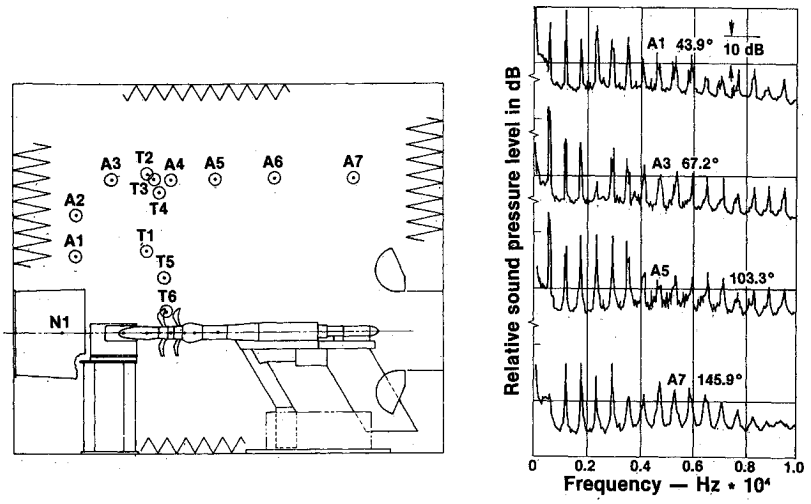

Fig. 3 Typical spectrum character of fore and aft microphone data.

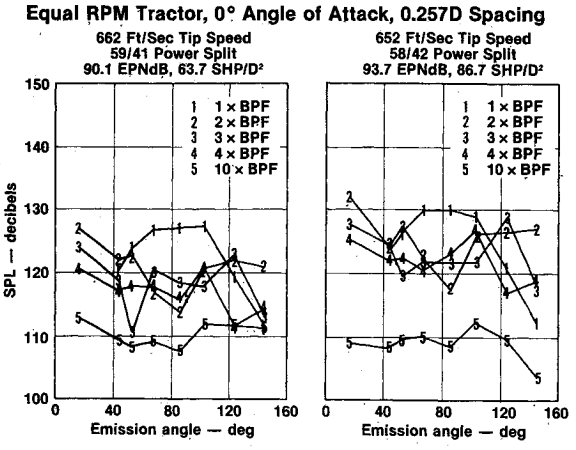

Fig. 4 Effect of power at constant tip speed.

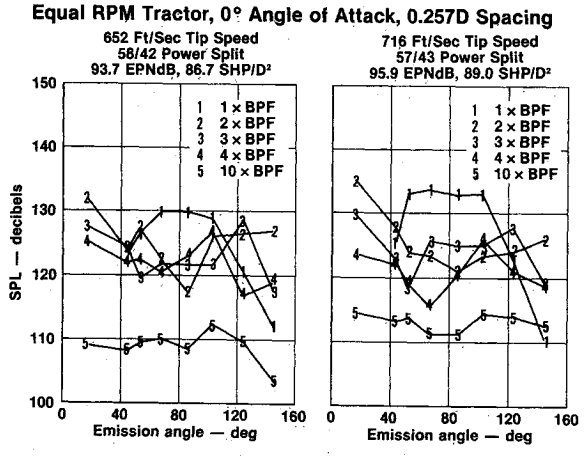

Fig. 5 Effect on tip speed at constant power.

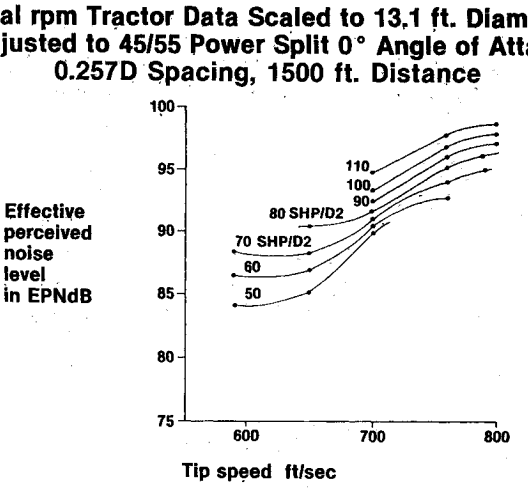

Fig. 6 Free-field effective perceived noise level trends.

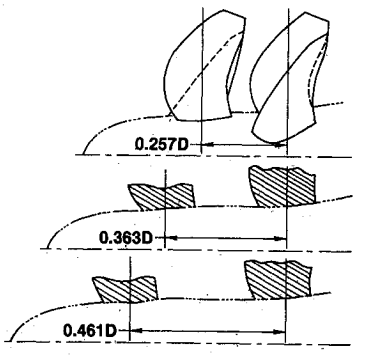

Fig. 7 Rotor-to-rotor spacing test configurations.

13.1 ft diam prop fan at a distance of 1500 ft. The power split for this curve is 45% at the front and 55% at the rear rotor. It can be seen that noise levels decrease as tip speed and SHP/D^2 are reduced. As the tip speed is reduced to 600 ft/s, the levels gradually reach a minimum. At tip speeds between 650 and 750 ft/s, the levels increase substantially, but at higher tip speeds the increase in level is not as great. From this figure it can be seen that it is important to operate at tip speeds between 600 and 650 ft/s at the lowest SHP/D^2 to achieve the lowest noise levels relative to Federal Aircraft Regulation Part 36 (FAR 36) limits.

Rotor-Rotor Spacing and Angle-of-Attack Effects

Figure 7 shows the rotor-rotor spacings for the test. As shown, the spacing is the nondimensional ratio of pitch-change axis to pitch-change axis distance divided by prop-fan diameter D. Nondimensional spacings from 0.257 to 0.461D were tested. In Fig. 8 the effect on effective perceived, noise level of rotor-rotor spacing at 0 deg angle of attack is shown in the three vertical bars at the left of each grouping. The bar at the right of each group is the 0.257D minimum spacing data at

an angle of attack 4 deg (axis of propfan rotation at 4 deg relative to the tunnel centerline). For each test point, the SHP/D^2 and tip speed is indicated. The power split from the front to rear rotor is 56/44 for each case shown. The effective perceived noise level is calculated assuming no ground reflection effects. In general, it can be seen that increasing the tip speed and the SHP/D^2 causes an increase in the effective perceived noise level. Inspection of the trends of noise with increased spacing shows generally small effects of less than 0.5 dB as the spacing is increased from 0.257 to 0.461 diameters. This result is confirmed in other data that generally showed small effects of rotor-rotor spacing. The far-left bar compared to the far-right bar in each grouping indicates the effect of angle of attack. In this case, the effect of angle of attack is less than 4 dB. Other data indicate that the average effect of angle of attack is about 3.5 dB.

Figure 9 shows a sample fore and aft directivity for 37.8 SHP/D^2, 633 ft/s tip speed and a 49/51 power split. The effect of rotor-rotor spacing on the harmonic directivity is indicated. It can be seen that the blade passage frequency directivity does not change; however, the directivity for the second harmonic of the blade passage frequency does change somewhat as spacing is changed. The most significant change is the increase in higher harmonic level in the forward portion of the directivity for emission angles from 20 to 65 deg.

Figure 10 shows a sample of the effect of angle of attack for a 37.8 SHP/D^2, 633 ft/s tip speed case. It can be seen that blade passage frequency increases substantially as the angle of attack changes from 0 to 4 deg. The levels fore and aft of the plane of rotation at two-times blade passage frequency also increase in level. At other harmonics the levels also increase and change in directivity as angle of attack is changed from 0 to 4 deg.

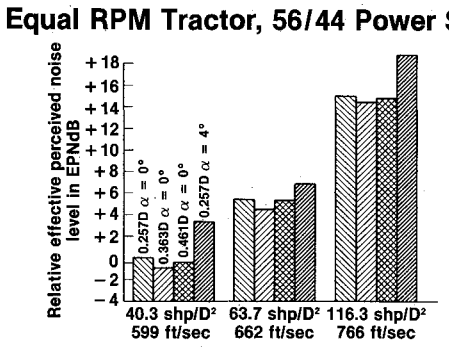

Fig. 8 Effect of power, tip speed rotor-rotor spacing, and angle of attack on scaled EPNdB.

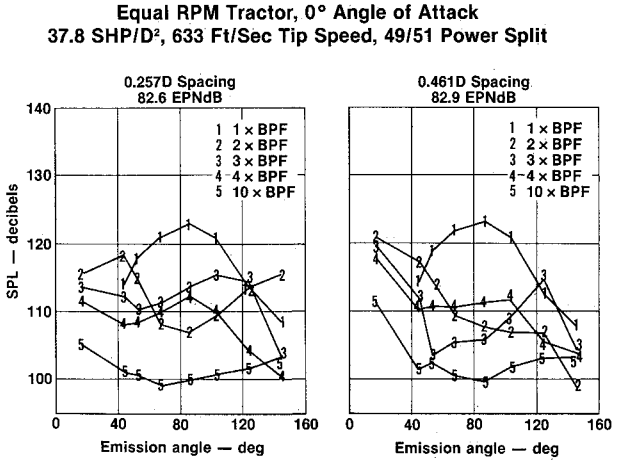

Fig. 9 Effect of rotor-rotor spacing.

In addition to fore and aft directivities, the transverse directivity was also measured. The convention used is shown at the left of Fig. 11. It is based on an aircraft height of 800 ft as might be appropriate for the sideline location of FAR 36 certification. For this geometry, the angle relative to the horizontal is 28.5 deg on the starboard side and 151.5 deg on the port side. Figure 11 also shows a sample of transverse directivity for 4 deg angle of attack that corresponds to the 4 deg angle of attack fore and aft directivity data shown in Fig. 10. It can be

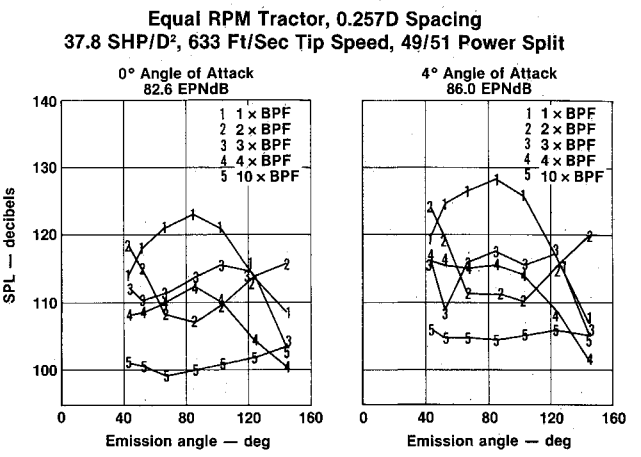

Fig. 10 Effect of angle of attack.

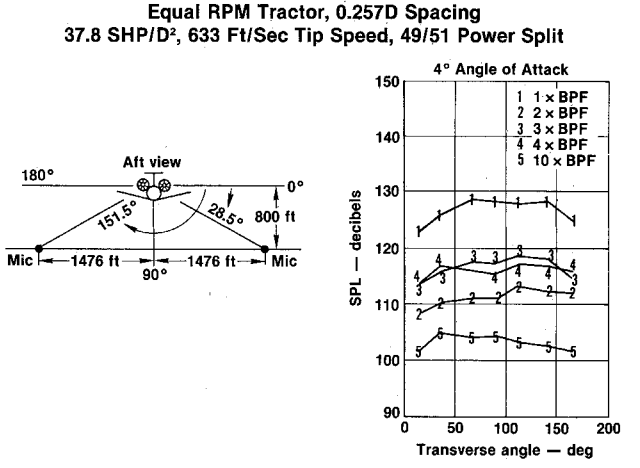

Fig. 11 Transverse effect of angle of attack.

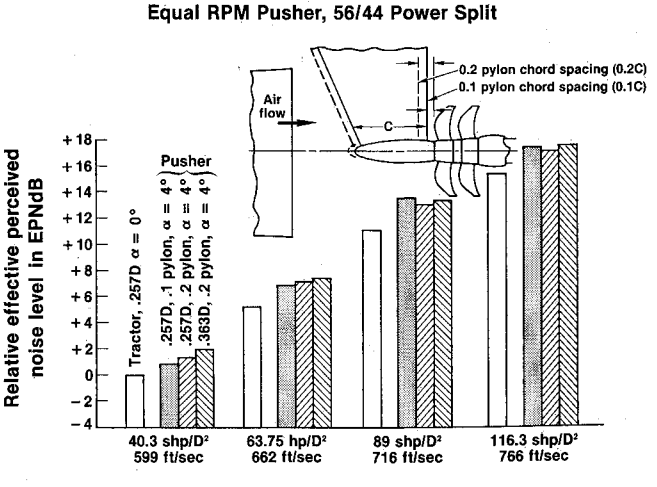

Fig. 12 Effect of power, tip speed, pylon and rotor-rotor spacing, and angle of attack on scaled EPNdB.

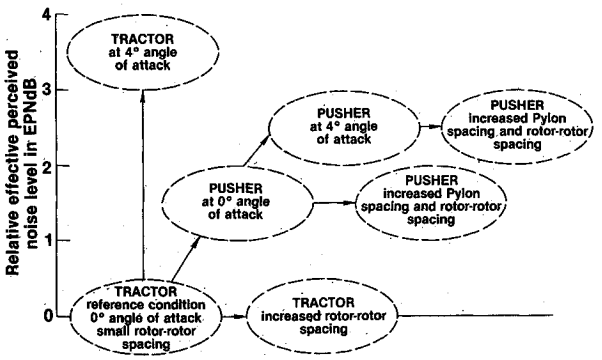

Fig. 13 Effects of configuration variables on effective perceived noise level.

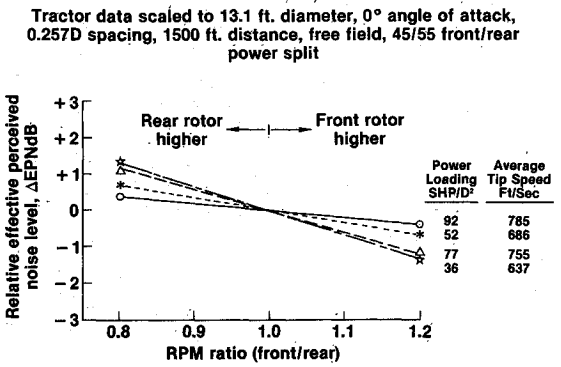

Fig. 14 Effect of front-to-rear rpm ratio on EPNdB.

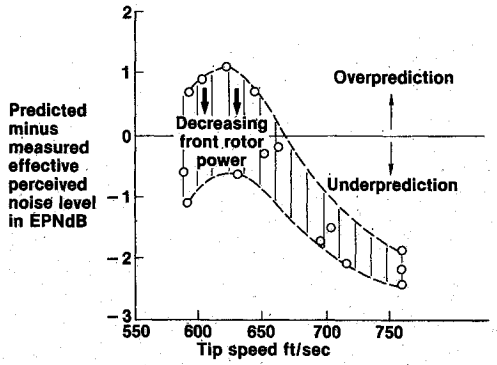

Fig. 15 Accuracy of predictions.

seen that there is some transverse effect of angle of attack. The noise levels at 15 and 165 deg are lower in level than at other locations. This is as expected in that conventional propeller data show the greatest increase in noise directly under the flight path with less effect on the sideline. This is the result of nonuniform loading of the blades due to the angle of attack.

Pusher Pylon Spacing and Angle-of-Attack Effects

In Fig. 12, a sample of the data showing the effects of pylon and angle of attack for the pusher configuration is presented. In the figure, the geometry of the pylon and the definition of spacing of the pylon relative to the front rotor are defined. Two pylon chord spacings were tested, one at 0.1 chord and the other at 0.2 pylon chords.

In Fig. 12, the EPNdB for the tractor at 0 deg angle of attack is compared with different pusher configurations at a 4 deg angle of attack. This is an indication of the installation effects that would occur for an aircraft. The 0 deg tractor is a pure axisymmetric case with no inflow disturbances (as might be found in a facility such as the Acoustic Research Tunnel). The 4 deg angle-of-attack pusher data is indicative of the level that would be achieved for an airplane at takeoff or approach where there is some angle of attack. It can be seen that the increase in tip speed and SHP/D^2 increases the level of the noise. Comparing the tractor at 0.257 spacing at 0 deg angle of attack with the pusher at 0.257 and 0.1 pylon spacing shows the effect of angle of attack at the minimum pylon spacing. The comparison with the next bar on the right shows the effect of increasing the pylon spacing to 0.2. The comparison within the pusher data shown is indicative of the small effect of the pylon spacing and rotor-rotor spacing for a given tip speed and power loading. In this figure, the greatest increase in pusher effect at 4 deg angle of attack vs tractor at 0 deg angle of attack is found with the 0.1 pylon spacing. This difference is approximately 2.5 dB. As the pylon spacing is increased, the penalty for pusher operation varies by a small amount. Also, as the spacing between the front and the rear rotor is increased, the penalty varies by a small amount.

Several data points were chosen to compare the effects of various test configurations on noise levels. Figure 13 summarizes the findings in terms of incremental EPNdB values relative to those of the tractor at 0 deg angle of attack and minimum spacing ($0.257D$) configuration. The figure indicates that:

1) Rotor-rotor spacing has little effect on noise in the tractor mode of operation.

2) Tractor 4 deg angle of attack adds approximately 3.5 dB relative to noise at 0 deg angle of attack.

3) Pusher 0 deg angle of attack adds approximately 1.5 dB relative to tractor at 0 deg angle of attack.

4) Increasing angle of attack from 0 to 4 deg increases noise levels on the order of 1 dB in the pusher mode of operation.

5) Pylon spacing and rotor-rotor spacing has little effect in the pusher mode of operation in the 0 and 4 deg angle-of-attack cases.

Effects of Operating the Front and Rear Rotors of the Tractor Configuration at Different Revolutions Per Minute

A summary of the effect of rpm ratio with a constant power split between rotors is shown in Fig. 14. Information for four power loadings and average tip speeds (the average of the front and rear rotor tip speeds) is shown with the front rotor operating 20% higher or lower than the average tip speed. It can be seen that operating the front rotor at higher tip speed results in consistently lower noise levels. The smallest benefits occur at high average tip speed and high power loadings.

Comparison of Predictions and Measurements

The accuracy of Hamilton Standard predictions vs measurements is reported in this section. The prediction procedure is theoretically based[3] and calculates the steady-loading (dipole) and thickness (monopole) noise of the front and rear rotor and the aerodynamic interaction noise at the rear rotor due to the potential and viscous wakes of the front rotor. The method calculates the directivity of each harmonic of blade passage frequency and also the effective perceived noise level. In general, the agreement of predicted and measured harmonic directivities has been found to be excellent at blade passage frequency. At higher harmonics, where the noise is caused by aerodynamic interaction between the two rotors, the noise is also well predicted.

The general agreement of predictions and measurements on an effective perceived noise level basis is shown in Fig. 15. The points shown are for different power loadings and different tip speeds. It can be seen that the measured levels are well predicted (within 1 EPNdB) from 590 to 670 ft/s tip speed with some underprediction at higher tip speeds. There is some tendency to underpredict the noise as the front rotor power is reduced, but this error is generally less than 1 dB.

Conclusions

The following conclusions are drawn from the test results:

1) General conclusion. The noise spectrum of counter-rotation prop fans was found to be rich in higher frequency harmonics of blade passage frequency due to aerodynamic interaction between the two rotors. Aerodynamic interaction noise was a significant contributor to the spectra fore and aft of the plane of rotation.

2) Tractor at 0 deg angle of attack. Levels of all harmonics of the spectrum generally increased with increasing loading and tip speed.

3) Tractor rotor-rotor spacing effects. In the tractor mode of operation, scaled EPNdB effects of rotor-rotor spacing were negligible.

4) Pusher at 4 deg angle of attack vs tractor at 0 deg angle of attack. In the pusher mode of operation, the combined pylon and angle of attack effect raised the scaled EPNdB levels of the tractor at 0 deg by approximately 2.5 dB. Increasing spacing between the pylon and front rotor or between rotors generally affected scaled EPNdB levels by a negligible amount.

5) Unequal rpm effects. For a tractor installation, with 45/55 power split, a lower noise was achieved when the front rotor was operating at a higher speed than the rear rotor.

6) Predictions vs measurements. Current predictions of EPNdB agree well with scaled data in the 590 to 670 ft/s tip speed range with some tendency to underpredict levels at higher tip speeds. As power absorption is biased toward the rear rotor, there is some evidence of underprediction.

Acknowledgments

The information reported was obtained under NASA Contract NAS3-24222. The authors wish to express their thanks for NASA approval to publish the results of the test. McDonnell Douglas Corporation support of the program, by providing the pylon and nacelle and other test equipment, is also acknowledged. The authors also wish to thank all of their colleagues, both at Hamilton Standard and United Technologies Research Center, for their enthusiastic support of the very demanding test reported here. It was an outstanding team effort by all who participated.

References

[1]Wainauski, H. S., "Aerodynamic Performance of a Counter Rotating Prop-Fan," AIAA Paper 86-1550, June 1986.

[2]Schlinker, R. H. and Amiet, R. K., "Experimental Assessment of Theory for Refraction of Sound by a Shear Layer," NASA CR-14359, 1978.

[3]Hanson, D. B., "Noise of Counter Rotation Propellers," AIAA Paper 84-2305, Oct. 1984.